An Experimental Direct Model for the Sky Temperature Evaluation in the Mediterranean Area: A Preliminary Investigation

Edoardo De Cristo [1,2], Luca Evangelisti [1,*], Claudia Guattari [3] and Roberto De Lieto Vollaro [1]

1 Department of Industrial, Electronic and Mechanical Engineering, Roma TRE University, Via Vito Volterra 62, 00146 Rome, Italy; edoardo.decristo@uniroma3.it (E.D.C.); roberto.delietovollaro@uniroma3.it (R.D.L.V.)
2 Department of Engineering, Niccolò Cusano University, Via Don Carlo Gnocchi 3, 00166 Rome, Italy
3 Department of Philosophy, Communication and Performing Arts, Roma TRE University, Via Ostiense 139/10, 00154 Rome, Italy; claudia.guattari@uniroma3.it
* Correspondence: luca.evangelisti@uniroma3.it

Abstract: Since the beginning of the 20th century, many studies have focused on the possibility of considering the sky as a body characterized by an apparent temperature, and several correlations to quantify the apparent sky temperature have been proposed. However, the different models were obtained for specific meteorological conditions and through measurements at specific sites. The available models do not cover all locations in the world, although the evaluation of the sky temperature is fundamental for estimating the net radiative heat transfer between surfaces and the sky. Here, experimental data logged from a regional micrometeorological network (in Italy, within the Lazio region) were processed and used to identify an empirical model for the estimation of the sky temperature in the Mediterranean area. Data relating to atmospheric infrared radiation were used to compute the sky temperature, aiming at identifying a direct correlation with the ambient temperature. Climatic data acquired during 2022 were processed. The proposed correlations were compared with other models available in the literature, including the standard ISO 13790. This study proposes an annual-based direct correlation in its initial phase, demonstrating a superior fit to the measured data compared to well-known direct empirical models from the literature. Subsequently, quarterly-based correlations are introduced further in a secondary phase of the work to improve the model's adaptation to experimental observations. The results reveal that quarterly-based correlations improve goodness-of-fit indexes compared to annual-based and well-known direct empirical correlations. Finally, a detached building was modeled via a dynamic code to highlight the influence of different correlations on annual energy needs.

Keywords: sky temperature; empirical model; experimental data; building energy simulation

1. Introduction

Addressing the global climate emergency requires innovative approaches and technologies to minimize human impact. It is essential to prioritize reducing reliance on non-renewable energy sources and cutting greenhouse gas emissions.

These priorities were acknowledged as part of the 2030 Agenda for Sustainable Development, a program of action endorsed in September 2015 by the governments of all 193 member countries of the United Nations [1]. It identifies 17 Sustainable Development Goals, among which are the fight against climate change and the mission of inclusive, safe, long-lasting, and sustainable cities and human settlements [2].

Despite energy efficiency policies in Europe, it is worth observing that the residential sector still accounts for about 40% of the overall energy usage and over a quarter of CO_2 emissions [3,4]. Among the main items of energy end uses, summer and winter air conditioning stand out [5]. Within cities, the first one improves the increasingly significant phenomenon of the so-called urban heat islands [6,7]. In countries characterized by hot

climates, cooling is a driving factor in the demand for electricity. Therefore, much attention is paid to research in the field of materials intended for passive radiative heat dissipation. These materials allow thermal energy to be transferred from surfaces toward external space passively, i.e., without demanding any energy input to work [8]. This heat transfer occurs through a radiative transmission mechanism. It is well known that this is the fastest heat transfer process, and solar radiation reaches the Earth's surface. All bodies characterized by a temperature above absolute zero continuously emit energy in the form of electromagnetic radiation, caused by molecular stirring. Thermal radiation encompasses the wavelengths of the electromagnetic spectrum that can heat a body upon absorption, ranging from 0.1 μm to 100 μm.

When considering surfaces such as building components, photovoltaic panels, or solar thermal collectors, it is necessary to consider the radiative heat transfer between them and the environment. The exchange of longwave infrared radiation between a surface and the sky depends on the specific exposure of the surface. This can be influenced by the slope, the presence of other bodies, and the temperature of the sky. The heat transfer with the sky vault is associated with the sky longwave radiation, which needs to be accounted for through the sky temperature concept. The sky temperature is the average of the ground temperature and the upper troposphere, where water vapor is much less abundant. Therefore, it does not represent the actual temperature of the sky but rather indicates that the sky is significantly warmer than space and cooler than clouds [9].

Urban areas exhibit significant spatial variations in terms of air temperature and shortwave radiation, influenced by factors such as surface cover, building heights, and green space percentage. These variations are crucial in shaping the urban climate and affect urban resilience [10]. Therefore, a comprehensive understanding of urban climate conditions from mesoscale [11,12] and microscale [13,14] perspectives is essential.

All this can be related to the building sector. Heat transfers between buildings and the environment occur through conduction, convection, and radiation. These heat exchanges are nowadays quantified through simulation software able to compute the energy needs for heating and cooling on a monthly or hourly basis. As mentioned before, the building sector in Europe is responsible for high energy consumption and polluting emissions. Consequently, detailed models are useful for simulating the thermal behavior of inefficient old buildings and testing the effects of energy retrofit solutions.

The net radiative heat flux (q_{rad}) between a building component and the sky vault can be computed by applying the following formula [15,16]:

$$q_{rad} = \varepsilon \sigma F_{sky} \left(T_s^4 - T_{sky}^4 \right) \tag{1}$$

where the emissivity of the building surface is represented by ε, F_{sky} is the sky view factor, and T_s is the surface temperature of the building component. Sky temperature (T_{sky}) is the average temperature of the sky. At the horizon, the sky temperature is equal to the ambient temperature. On the other hand, the coldest part of the sky is the portion above. Using a view factor value of 0.5 for vertical surfaces in energy simulations is a widely employed approach. This approach assumes a constant sky temperature, simplifying the computational process. However, this approach cannot be considered entirely representative [17]. To calculate the net radiative heat flux, the sky temperature is fundamental, but it is not measured by weather stations. Consequently, correlations have been developed to obtain the sky temperature as a function of climatic parameters.

Nowadays, energy simulation software programs exploit models for estimating the temperature of the sky [18]. Research in the literature shows that since the beginning of the 20th century, many studies have focused on the possibility of considering the sky as a body characterized by an apparent temperature. Based on this, several correlations to quantify the apparent temperature of the sky were proposed [19–23].

Analyzing the available sky temperature models in the literature, it is possible to distinguish empirical and detailed models [17]. Alongside them, it is also possible to mention the standard ISO 13790 [24].

Within empirical models, correlations for clear-sky and cloudy-sky conditions can be observed. These correlations are based on direct measurements of infrared radiation. Moreover, within these two classifications, it is possible to recognize direct models and sky emissivity models: The first ones allow for the calculation of the sky temperature by using only the ambient temperature (T_{amb}); the latter ones need the sky emissivity (ε_{sky}) evaluation to compute the sky temperature. This means that the sky is considered a gray body, characterized by an apparent emissivity. Consequently, atmospheric radiation (q_{sky}) can be calculated according to $q_{sky} = \varepsilon_{sky} T_{amb}^4$. By contrast, by considering the sky as a black body, atmospheric radiation can be computed by applying the well-known Stefan–Boltzmann law as a function of a sky emissivity equal to 1 and the fourth power of the apparent thermodynamic temperature of the sky. By comparing the two approaches, it is possible to obtain the equation $T_{sky}^4 = \varepsilon_{sky} T_{amb}^4$.

Several direct and sky emissivity models for clear-sky conditions were presented in the literature.

In 1963, Swinbank [25] introduced a novel clear-sky direct model that allowed for the estimation of sky temperature solely based on ambient temperature data. The Swinbank correlation was derived by averaging the values of elevation and humidity. Later, in 1982, Garg [26] proposed a different clear-sky direct model for estimating the sky temperature. Based on experimental investigations conducted in Australia, the author proposed a correlation for directly computing the sky temperature simply by subtracting 20 °C from the ambient temperature observations. In 1918, Angström [27] presented the first clear-sky emissivity model. Based on an extensive set of observations performed in Algeria (Bassour), the proposed correlation ensures the computation of the sky's emissivity, considering the prevailing atmospheric vapor pressure at any given time. Starting from climate data recorded in the United Kingdom in 1932, Brunt [28] introduced a novel sky emissivity correlation valid for clear-sky conditions. The correlation estimates the sky emissivity based on the square root of water vapor partial pressure and two empirical dimensionless coefficients (a = 0.52 and b = 0.065). The correlation assumes that the sky emissivity varies linearly with the said parameter. After two years of observations in Ohio, USA, Sloan et al. [29] developed an alternative clear-sky emissivity model in 1956 to estimate the sky emissivity using only absolute humidity (AH) data. In 1969, Idso and Jackson [30] presented another clear-sky emissivity correlation for assessing sky emissivity under clear-sky conditions, relying only on air temperature values. From 1982 to 2004, several clear-sky emissivity models were proposed for estimating sky emissivity as a function of the dew point temperature only [31–35].

On the other hand, different direct and sky emissivity models were proposed over the years considering the impact of clouds on the calculation.

Among these, there is the simplified and practical direct cloudy-sky correlation proposed by Dreyfus [36] in 1960. This correlation allows for estimating the sky temperature by imposing the identity between sky and ambient temperatures. In 1967, Whillier [37] introduced an alternative simplified direct cloudy-sky model, offering a user-friendly method for computing the sky temperature by subtracting 6 °C from the ambient temperature observations. In 1987, after analyzing climatic data from 68 cities in the US, Fuentes [38] modified the Swinbank [25] model and proposed an alternative direct cloudy-sky correlation for estimating the sky temperature starting from ambient temperature data. With the undeniable variability of sky conditions and the consequential impact of cloud presence on infrared radiation observations, various cloudy-sky emissivity models have been proposed in the literature over the years. These models aim to adjust clear-sky correlations and extend their applicability to cloudy conditions. Among these, the Clark and Allen [39] correlation, introduced in 1978, remains in use in the dynamic code EnergyPlus 22.1.0 [40]. The authors presented a correction factor (C_a) to account for the variation of sky cover in

sky emissivity computation. The correction factor varies with clear-sky conditions (N) and is the ratio of observed cloud sky atmospheric radiation to estimated clear-sky atmospheric radiation. In 1980, Kasten and Czeplak [41] proposed an alternative emissivity model for cloudy skies, which employs a cloudiness factor (CF) to account for varying sky conditions. Specifically, a CF value of 0 represents a clear-sky scenario, whereas a CF of 1 signifies an utterly overcast sky. In 1984, Berdahl and Martin [42] introduced a sky emissivity correlation based on the cloud sky fraction (f_{cloud}), which can be compared to the Kasten and Czeplak correlation [41]. An f_{cloud} index of 0 represents a clear-sky condition, while a value of 1 represents an overcast sky scenario.

Detailed models, in contrast, analyze the atmospheric components to assess gases' radiative characteristics and calculate infrared radiation. These sophisticated models necessitate comprehensive data on pressure, temperature, density relative to elevation, gas concentration, and spectral absorption coefficients. In 1961, Bliss [43] introduced one of the most practical correlations among the detailed models. This correlation allows for the estimation of the sky's emissivity based solely on dew point temperature data.

More exhaustive information on the most well-known models in the literature for estimating the temperature of the sky is reported in [17].

Lastly, the formulas reported in ISO 13790 identify a simplified approach, with a sky temperature value predictable by subtracting a specific constant from the ambient temperature, based on the climatic area (temperate, sub-polar, or tropical). The classification of available models is shown graphically in Figure 1.
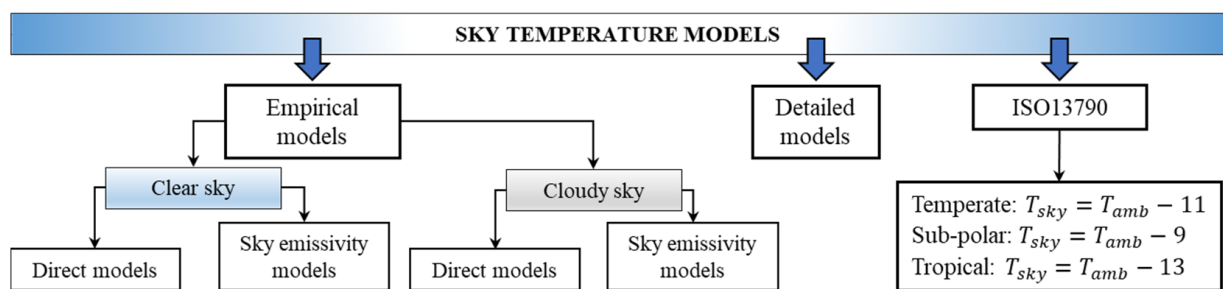

Figure 1. Existing sky temperature models.

The correlations proposed over time are related to local climatic conditions and measurements conducted at specific locations. Such variations have been an essential factor in the development of new models. In 2019, Evangelisti et al. [17] provided a literature review of the available formulas for the evaluation of the sky temperature and sky emissivity, considering models suggested since 1918, and also provided a comparison among them. The current models vary substantially in form and complexity. The authors concluded that the best formula for the Mediterranean area cannot be identified due to the lack of equations for all areas of the World.

For this reason, this work, which can be identified as a follow-up of [17], aimed to suggest a new correlation for the Mediterranean area starting from experimental data acquired by a micrometeorological network installed in the Lazio region (Italy). Climatic data logged in 2022 were processed to provide a preliminary new direct model and an alternative methodological approach in terms of data processing for the sky temperature estimation. Moreover, the proposed correlation was compared with others available in the literature [36–38], including the ISO 13790 standard. Finally, a detached building was modeled via dynamic simulation software to assess the effect of different correlations on annual energy needs for air conditioning.

The preliminary direct model proposed here could be considered an alternative solution to the standardized model provided by ISO 13790, widely used in engineering practices for assessing sky temperature in regions with temperate climates, such as Italy. Finally,

the methodological approach presented here can be applied by considering other datasets related to different geographical areas for the requirements of calibrated energy models.

2. Materials and Methods

2.1. The Micrometeorological Network

A micrometeorological network was designed by ARPA Lazio [44] in 2012 to support the assessment and forecasting of air quality within and near Rome (see Figure 2a,b). The stations are equipped with meteorological sensors for measuring environmental temperature, humidity, pressure, and precipitation, associated with sonic anemometers, pyranometers, and pyrgeometers. The measurement sites comply with the indications of the World Meteorological Organization. Figure 2b shows the different positions of the weather stations. For this work, meteorological conditions recorded in station number 3 in Figure 2b were selected based on the availability and completeness of the climatic data.

Figure 2. (**a**) Italy; (**b**) positions of the meteorological stations within and around Rome.

2.2. Methodology

The infrared atmospheric radiation and ambient temperature data were acquired in 2022. A preliminary data cleaning procedure was accomplished via the programming and numeric computing platform MATLAB R2024a [45]. The climatic data were organized within tables, and time intervals relating to missing data were excluded. The measured longwave atmospheric radiation (q_{sky}) was used to compute the sky temperature by using the following equations:

$$q_{sky} = \sigma T_{sky}^4 \tag{2}$$

$$T_{sky} = \left(\frac{q_{sky}}{\sigma} \right)^{\frac{1}{4}} \tag{3}$$

where σ is the Stefan–Boltzmann constant, and T_{sky} is the temperature of the sky.

By applying Equation (3), a preliminary direct model was identified as a function of the ambient temperature (T_{amb}). Employing the available climatic data, the proposed model allows for expressing the sky temperature as a function of the ambient temperature, in the form of a straight-line equation ($T_{sky} = mT_{amb} + c$).

The methodological approach is characterized by two steps. Within the first step, the data recorded for all of 2022 were processed following an annual-based approach (considering the measured longwave atmospheric radiation and ambient temperatures acquired during the whole year). The following goodness-of-fit indexes were computed for

assessing the reliability of the proposed empirical correlation: coefficient of determination (R^2), normalized mean bias error (NMBE), and the coefficient of variation of the root mean square error (CV(RMSE)).

The coefficient of determination (R^2) is a frequently employed statistical parameter, ranging from 0 to 1, for assessing model uncertainty [46]. This index gauges the proximity of simulated values to the regression line of measured values. A higher value indicates a closer alignment between simulated and measured values, while a lower value indicates a weaker correspondence. According to the ASHRAE Guidelines [47] and IPMVP [48], the R^2 value should be at least 0.75 for calibrated models. The coefficient of determination can be calculated as follows:

$$R^2 = \left(\frac{n \cdot \sum_{i=1}^{n} m_i \cdot s_i - \sum_{i=1}^{n} m_i \cdot \sum_{i=1}^{n} s_i}{\sqrt{\left(n \cdot \sum_{i=1}^{n} m_i^2 - \left(\sum_{i=1}^{n} m_i \right)^2 \right) \cdot \left(n \cdot \sum_{i=1}^{n} s_i^2 - \left(\sum_{i=1}^{n} s_i \right)^2 \right)}} \right)^2 \tag{4}$$

where n is the number of recorded observations, m_i is the i-th measured value, and s_i is the i-th simulated value.

The normalized mean bias error (NMBE) is a normalization of the mean bias error (MBE). MBE is a nondimensional bias measure between measured and simulated data defined as follows:

$$MBE = \frac{\sum_{i=1}^{n} (m_i - s_i)}{\sum_{i=1}^{n} (m_i)} \tag{5}$$

It is worth noting that the MBE is characterized by a cancellation effect, where a positive bias compensates for a negative bias. The NMBE can be calculated in the following manner:

$$NMBE = \frac{MBE}{\overline{m}} \times 100\% \tag{6}$$

where $\overline{m}$ is the mean of the measured values.

Finally, the coefficient of variation of root mean square error (CV(RMSE)) allows us to define how well a model fits the data by using offsetting errors between measured and simulated data. This index can be computed as follows:

$$CV(RMSE) = \frac{\sqrt{\sum_{i=1}^{N} (m_i - s_i)^2 / N}}{\overline{m}} \tag{7}$$

ASHRAE Guidelines 14 [49] define calibration as a process for reducing the uncertainty of a mathematical model by comparing the result simulated by the model (considering specific conditions) with data obtained from measurements. The accuracy of the calibration procedure can be assessed based on the monthly and hourly criteria reference values for the NMBE and CV(RMSE) furnished by ASHRAE Guidelines 14. The monthly NMBE is expected to be within ±5%, whereas the hourly NMBE should be within ±10%. In contrast, the monthly CV(RMSE) should be within ±15%, while the hourly CV(RMSE) should be within ±30%.

The obtained correlation was compared with the available direct models for cloudy-sky conditions, documented in Table 1, for computing sky temperatures, also taking into account the formula recommended by ISO 13790, currently used in engineering applications for estimating the sky temperature in geographical areas characterized by temperate climatic conditions.

Table 1. Empirical cloudy-sky direct models.

Model	Date	Equation
Dreyfus	1960	$T_{sky} = T_{amb}$
Whillier	1967	$T_{sky} = T_{amb} - 6$
Fuentes	1987	$T_{sky} = 0.037536 T_{amb}^{1.5} + 0.32 T_{amb}$
ISO 13790	2008	$T_{sky} = T_{amb} - 11$

Based on the obtained goodness-of-fit index values, an alternative approach was proposed in the second phase of the work. R^2 values were computed considering monthly, bimonthly, and quarterly approaches in order to identify the best solution for grouping the available experimental acquisitions. The bimonthly approach consisted of dividing the data into 2-month time intervals (January–February, March–April, and so on). On the other hand, in the quarterly breakdown approach, the data were grouped in 3-month time intervals (from January to March, from April to June, from July to September, and finally, from October to December).

Finally, the evaluation of the influence of different correlations on building energy needs for cooling and heating was assessed. A detached building was modeled via TRNSYS 16 simulation software, and the sky temperature correlations listed in Table 1 along with the proposed equations were applied.

In particular, the "TRN-Build" type was used for modeling two cubic-shaped structures characterized by different thermal insulation levels. The walls of the first building (labeled as B1) were made of solid bricks plastered on both sides. On the other hand, the second building (labeled as B2) had walls made of concrete and an external XPS layer, plastered on both sides. The thermophysical properties of the wall layers are listed in Table 2. A user-defined correlation based on the formula suggested by ISO 6946 [50] was set for external heat transfer convective coefficients:

$$h_c = 4v + 4 \tag{8}$$

where v is the wind speed.

Table 2. Thermophysical properties of the wall layers (from inside to outside).

Building	Layer	Thickness [m]	Thermal Conductivity [W/mK]	Mass Density [kg/m^3]	Specific Heat Capacity [J/kgK]
B1	Plaster	0.02	0.700	1400	1000
	Solid brick	0.58	0.770	1600	840
	Plaster	0.02	0.700	1400	1000
B2	Plaster	0.02	0.700	1400	1000
	Concrete	0.20	0.730	1600	1000
	XPS	0.06	0.034	50	1450
	Plaster	0.02	0.700	1400	1000

According to ISO 7730 [51], the heat gains from occupants of conditioned spaces were set equal to 65 W for sensible heat and 55 W for latent heat (low activity level). Moreover, the heat gain from the electrical apparatus was set equal to 140 W. The indoor temperature set points were 20 °C for heating and 26 °C for cooling.

On the other hand, the "TRNSYS Simulation Studio" was used for modeling the environment in terms of climatic conditions, and sky temperature was computed by applying both the specific "Type 69" (widely used as a standard component of the library and based on the Berdahl and Martin [42] formulation for computing the emissivity of the sky and thus the sky temperature) and the assembly function to insert the equations shown in Table 1 and the new ones proposed here.

The outcomes from all the considered approaches were analyzed and compared. Figure 3 shows the flowchart of the applied methodology.
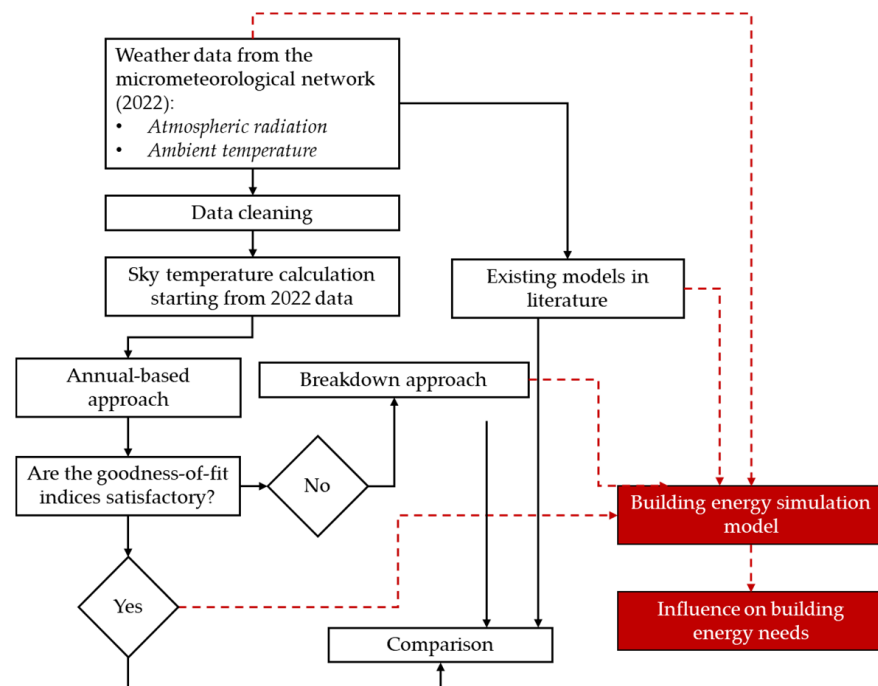
Figure 3. Diagram of the applied methodology: black lines refer to the first step of the research; red dotted lines refer to the second step.

3. Results and Discussion

3.1. Empirical Correlations for Estimating the Sky Temperature

As mentioned, climatic data in 2022 were collected from a weather station within the ARPA micrometeorological network in Lazio, Italy. Ambient temperature and infrared radiation data were analyzed to propose a new correlation for estimating the sky temperature in the Mediterranean area.

From the acquired q_{sky} data, the sky temperature values were computed by applying Equation (3) and used with T_{amb} data to identify the most suitable direct correlation for evaluating the sky temperature as a function of the ambient temperature. Figure 4 shows the new correlation (red line), also providing a comparison among the proposed function and the available equations proposed by Dreyfus (yellow line), Whillier (purple line), Fuentes (light blue line), and the ISO 13790 standard (gray line). The findings reveal that the proposed annual-based formula is more accurate in fitting the temperature data recorded in 2022 than the other ones. Among the well-known correlations available in the literature, the ISO 13790 equation seems to fit the observed climate conditions better. As illustrated, the linear regression procedure reveals an annual-based correlation characterized by an R^2 value slightly lower than 0.7. On the other hand, the NMBE and CV(RMSE) result in values equal to -7.9×10^{-13}% and -317.4%, respectively. The indexes were computed using the T_{sky} values derived from the experimental longwave radiation and the sky temperatures were computed by applying the function shown in Figure 4. Notably, while the NMBE value meets the calibration criteria outlined in ASHRAE Guidelines 14, the R^2 and CV(RMSE) values need improvement. Specifically, the coefficient of determination falls below 0.75, and the coefficient of variation of the root mean square error exceeds 30%.
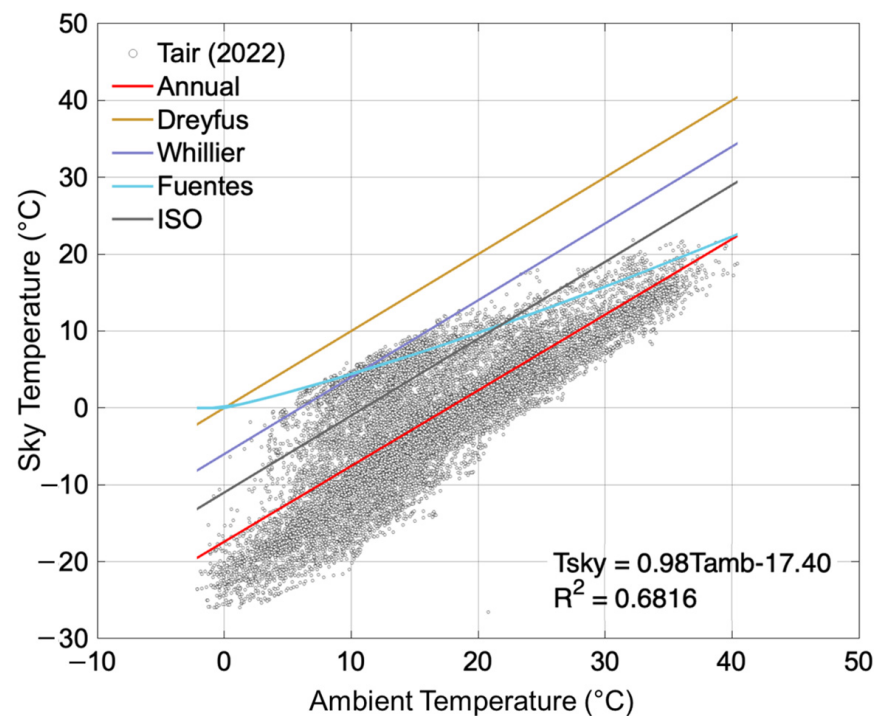
Figure 4. Comparison among the proposed annual-based empirical correlation and the other available correlations in the literature (Dreyfus [36], Whillier [37], Fuentes [38], and ISO 13790).

Despite the unsatisfactory indices, it is possible to observe that the preliminary suggested equation better estimates the sky temperature values based on experimental data. The proposed model is related to a methodological approach based on the processing of data that can be downloaded and managed by professionals, thus obtaining a specific equation as a function of the processed data. What has been stated is even more evident if a comparison is made with the other correlations in the literature.

The discrepancies in the results highlighted in Figure 4 are related to models derived from experimental measurements conducted in parts of the world other than the Mediterranean. In particular, the Whillier model was established in 1967, based on measurements conducted in the US, by correcting ambient temperature by 6 °C. On the other hand, the Fuentes model was identified in 1987, based on data measurements from 68 cities in the US, starting from the correlation proposed by Swinbank [25] and modifying it, employing a clearness index (this is the ratio between the measured solar radiation and the total solar radiation that could be received under completely clear-sky conditions). Finally, the Dreyfus model equals ambient and sky temperatures, thus obtaining higher sky temperature values than the other correlations.

Based on the acquired data, an analysis was conducted using monthly, bimonthly, and quarterly segmentation methods to determine the optimal approach for data organization. The R^2 values were then assessed to discern the most effective data-splitting strategy. Figure 5 depicts that the quarterly-based segmentation has superior accuracy, yielding higher R^2 values over extended periods. Conversely, the monthly segmentation exhibits reduced accuracy in representing the observed climate conditions for 2022 compared to the other segmentation methods.
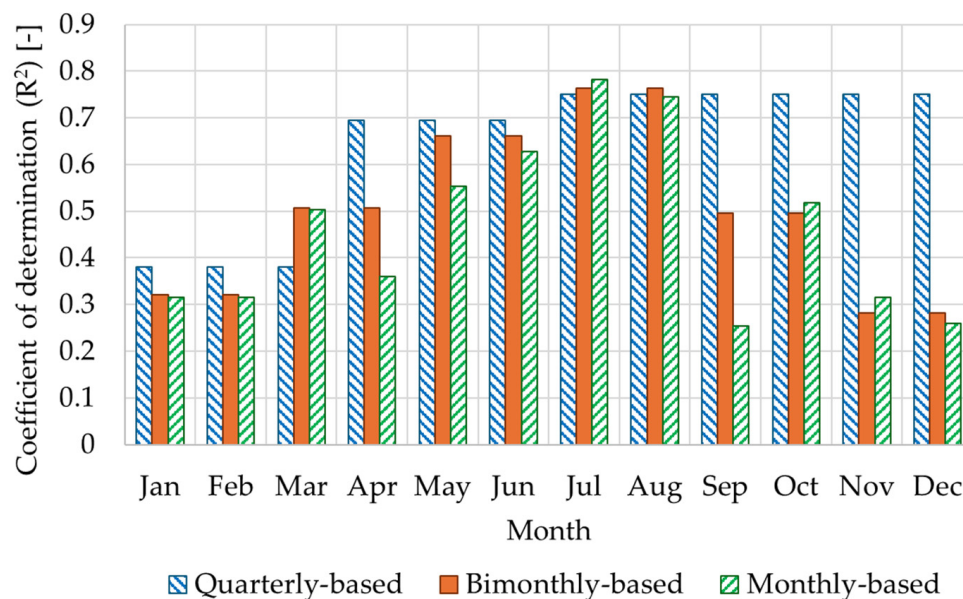
Figure 5. Comparison among the obtained coefficient of determination values by employing different data-splitting approaches.

Therefore, the data were organized using a quarterly breakdown method to derive distinct mathematical models for different periods of the year. Four quarterly correlations for estimating T_{sky} were identified, which are presented in Table 3.

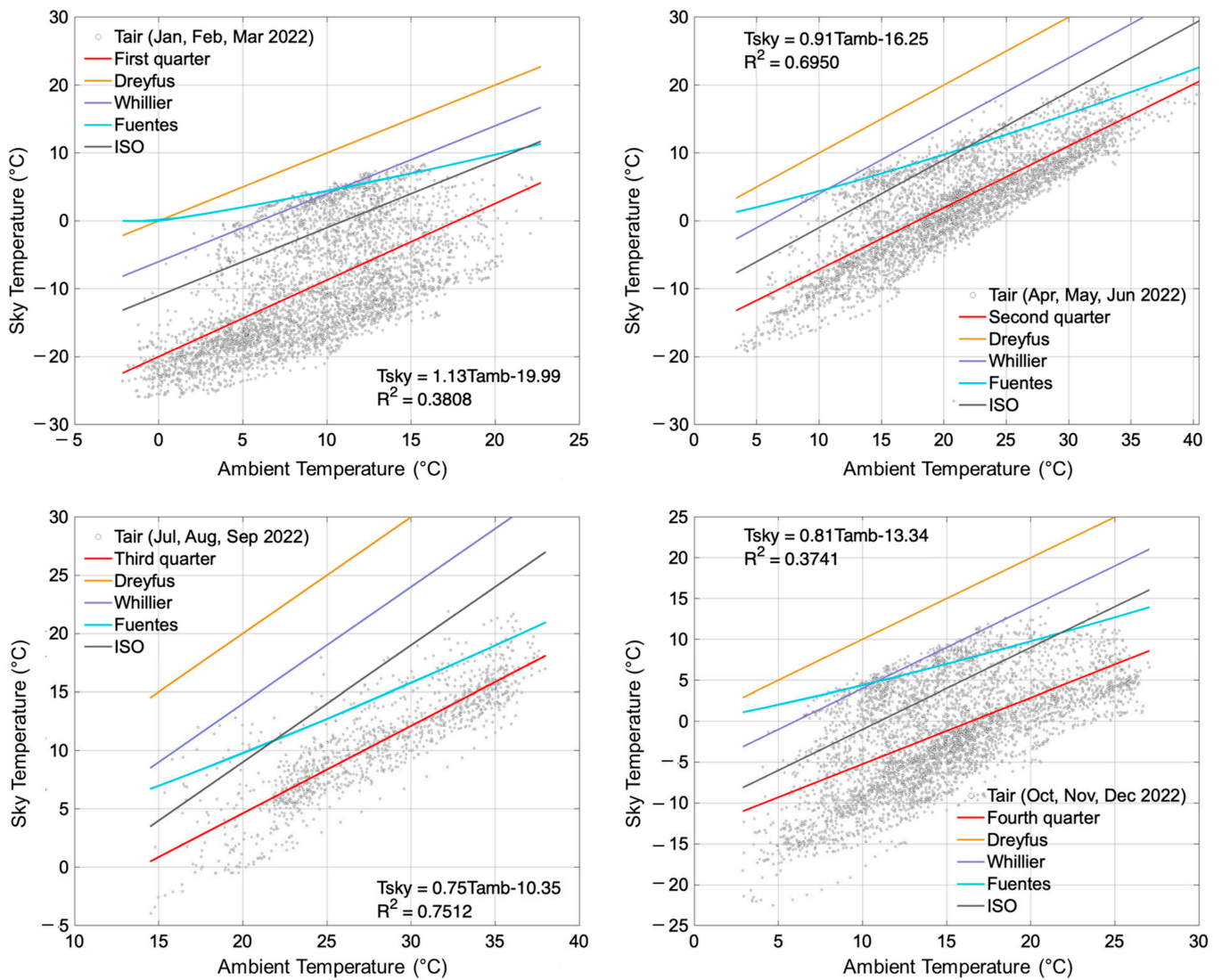**Table 3.** Quarterly-based correlations for calculating the sky temperature.

Quarter	From	To	Correlation
I	January	March	$T_{sky} = 1.13T_{amb} - 19.99$
II	April	June	$T_{sky} = 0.91T_{amb} - 16.25$
III	July	September	$T_{sky} = 0.75T_{amb} - 10.35$
IV	October	December	$T_{sky} = 0.81T_{amb} - 13.34$

Also in this step, sky temperature values were computed by employing the well-known cloudy-sky direct correlations listed in Table 1, and the outcomes were compared with those obtained from the proposed quarterly correlations (see Figure 6).

The accuracy of the proposed quarterly empirical formulas was evaluated by calculating the already mentioned goodness-of-fit indexes, obtaining quite improved values during the hottest months of the year (quarters II and III, that is, from April to September). The overall obtained indexes are shown in Table 4. The highest R^2 values can be observed during the second and third quarters. Being close to zero value, NMBEs always meet ASHRAE calibration criteria. By contrast, the CV(RMSE) index falls below 30% only in the third quarter. The obtained results demonstrate a more accurate estimation of T_{sky} during the summer season (July, August, and September) when the identified correlations are employed.

Table 4. R^2, NMBE, and CV(RMSE) for the quarterly-based approach.

Quarter	R^2 [−]	NMBE [%]	CV(RMSE) [%]
First (I)	0.38	3.69×10^{-13}	−68.70
Second (II)	0.69	1.44×10^{-14}	164.40
Third (III)	0.75	-1.28×10^{-13}	21.53
Fourth (IV)	0.37	-4.59×10^{-13}	−373.01

Figure 6. Comparison among the proposed quarterly-based correlations and the other available equations in the literature (Dreyfus [36], Whillier [37], Fuentes [38], and ISO 13790).

This approach allows us to progressively compute sky temperatures by applying different equations along the year as a function of the specific quarter. The reliability of the quarterly-based approach in estimating the T_{sky} values for all 2022 can thus be assessed by computing the goodness-of-fit indexes using all the 2022 T_{sky} values (calculated from the longwave radiation) as the measured data and all the 2022 T_{sky} values computed from the proposed quarterly-based correlations as the simulated values. According to this, Table 5 reports all the goodness-of-fit index values obtained using the quarterly-based correlations, Fuentes, and ISO 13790 models. Utilizing the quarterly-based correlations resulted in a high R^2 value compared to the previously discussed annual-based empirical correlation. However, it should be noted that the CV(RMSE) value failed to meet the calibration criteria proposed by ASHRAE. The small NMBE values observed can be attributed to the characteristics of our dataset and the methodology employed in our study.

Starting from the climatic data related to 2022, the proposed correlation outperforms the one suggested by ISO 13790 and Fuentes (i.e., the two correlations closest to the one proposed). This can be demonstrated by recalculating the goodness-of-fit indexes, considering ISO 13790 and Fuentes correlations as references for simulated sky temperatures (see Table 5). The quarterly-based approach allows us to obtain the best values of the indexes, even if they do not completely meet the criteria suggested by ASHRAE.

Table 5. R^2, NMBE, and CV(RMSE) considering ISO and Fuentes correlations as reference.

Correlation	R^2 [−]	NMBE [%]	CV(RMSE) [%]
Quarterly-based approach	0.70	-5.83×10^{-13}	−307.26
Fuentes	0.67	−552.02	−670.60
ISO 13790	0.68	−389.29	−502.34

3.2. Influence of Sky Temperature Correlations on Building Energy Simulations

TRNSYS 16 software was used for creating a model of a detached building, and different correlations for assessing the sky temperature were applied. Figure 7 shows the results in terms of annual heating and cooling energy needs, also providing a comparison between structures characterized by different thermal insulation levels (B2 was better thermally insulated than B1).
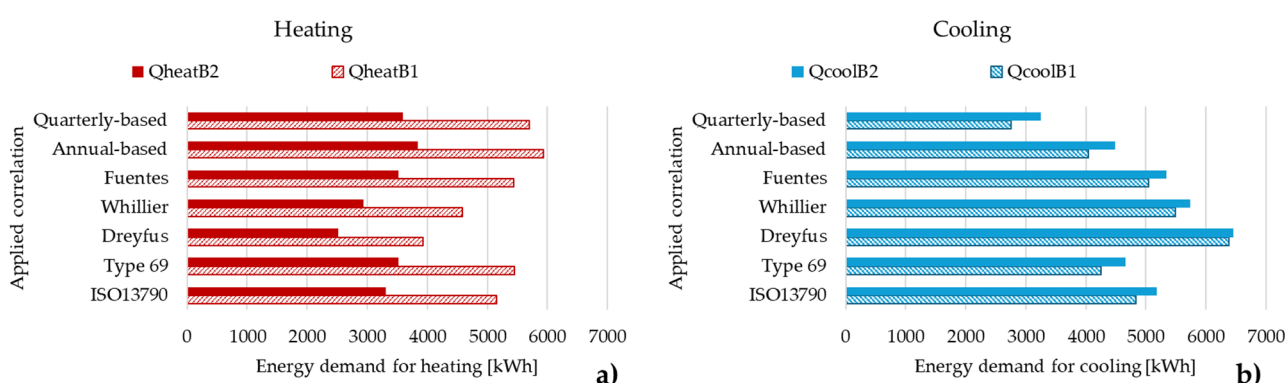
Figure 7. Annual heating (**a**) and cooling (**b**) energy demands.

For B1, heating energy demands ranged between 3926 kWh (obtained by applying the Dreyfus correlation) and 5929 kWh (obtained by applying the annual-based correlation). On the other hand, cooling energy demands ranged between 2748 kWh (found using the quarterly-based correlation) and 6378 kWh (found using the Dreyfus correlation).

For B2, the lowest heating energy demand (2519 kWh) was found by applying the Dreyfus correlation. By contrast, the highest value (3839 kWh) was obtained by applying the annual-based correlation. Considering cooling energy needs, the lowest value (3246 kWh) was found by applying the quarterly-based correlation, and the highest value (6454 kWh) was simulated using the Dreyfus equation. Considering the sky temperature equal to the ambient temperature, the Dreyfus equation resulted in the lowest heating energy needs and the highest cooling energy demands.

Taking ISO 13790 as a reference, the percentage differences computed using the different tested correlations are listed in Table 6. It is possible to observe the highest variations during summer, with values ranging from −35.28% to +50.20% for B1 and from −30.31% to 38.56% for B2.

Table 6. Heating and cooling percentage differences considering ISO 13790 as reference.

Correlation	QheatB1	QcoolB1	QheatB2	QcoolB2
Berdahl and Martin (Type 69)	5.88%	−12.18%	6.38%	−10.04%
Dreyfus	−28.02%	50.20%	−28.47%	38.56%
Whillier	−16.02%	29.42%	−16.52%	23.07%
Fuentes	−0.20%	18.88%	−0.15%	14.63%
Annual	8.70%	−4.93%	9.00%	−3.65%
Quarterly	4.46%	−35.28%	2.16%	−30.31%

In light of the newly proposed correlations for estimating sky temperature using a quarterly segmentation method, it is pertinent to compare them with ISO 13790 taking into account the quarterly-based approach as a reference. This can be useful because the Standard is widely employed in engineering practices to estimate sky temperature in regions with temperate climates, such as Italy. When comparing the results from the approach based on quarterly divisions with those derived from the simplified equation proposed by the ISO standard, differences in heating and cooling estimations are observed. Heating variations ranged from -9.58% (for B1) to -7.98% (for B2) while cooling variations ranged from 59.50% (for B2) to 75.94% (for B1).

4. Conclusions

In this work, experimental data acquired in 2022 by an Italian micrometeorological network were processed to identify a new direct model for the estimation of the sky temperature in the Mediterranean area. The proposed correlation was compared with other models available in the literature, including the standard ISO 13790. Finally, a detached building was modeled via TRNSYS to focus on the influence of different correlations on annual energy needs for heating and cooling.

A single correlation was primarily identified by processing data related to the whole year, obtaining an R^2 value slightly lower than 0.7, an NMBE equal to $-7.9 \times 10^{-13}\%$, and a CV(RMSE) of -317.4%. Given the unsatisfactory indexes, an approach based on the identification of multiple correlations for a single year was used, considering quarters. Thus, four equations were found, observing a clear improvement in the indicators only for the third quarter, related to the months of July, August, and September.

Despite the unsatisfactory indices, it is possible to observe that the preliminary identified equations better estimate the sky temperature values based on experimental data. The proposed model is related to a methodological approach based on the processing of climatic data that can be downloaded and managed by professionals, thus obtaining a specific equation as a function of the specific processed data.

However, by comparing the sky temperatures obtained from the radiation data with those calculated from the various mathematical models tested for the year 2022, large discrepancies were identified. Nevertheless, is noteworthy that the direct models available in the literature (including ISO 13790) can be applied for simulating the thermal behavior of buildings and engineering devices based on average climatic conditions (e.g., in the case of energy certification of buildings), while for considering energy retrofit strategies for existing structures, calibrated dynamic simulations are fundamental based on specific thermal boundary conditions. The approach proposed here allows for the identification of the best sky temperature correlation for the time and area under investigation (i.e., the area in which the building is located and the period for which there are measured data useful for calibrating the energy model), based on experimental data.

The limits of this work are related to (i) data processing based on the year 2022 only, (ii) data processing based on only one weather station, and (iii) the impossibility of having identified a direct correlation (therefore simple to use) for the coldest months of the year. These aspects will require further efforts during future research developments.

It is also important to observe that the lack of equations for all regions of the world leads to the unfeasibility of defining the most suitable formula. However, model comparison can be useful to guide user choice in energy simulations and engineering applications.

Future developments will concern the analysis of a greater volume of data, deriving from more weather stations and considering more years. Furthermore, a more accurate statistical data analysis will be pursued, considering both air temperature and relative humidity trying to identify models characterized by more satisfactory index values.

References

1. United Nations. Agenda 2030. Available online: https://Sdgs.Un.Org/2030agenda (accessed on 29 November 2023).
2. United Nations. The 17 Goals. Available online: https://Sdgs.Un.Org/Goals (accessed on 29 November 2023).
3. IEA Buildings. Paris, 2022. Available online: https://www.Iea.Org/Reports/Buildings (accessed on 29 November 2023).
4. *Directive 2010/31/EU of the European Parliament and of the Council of 19 May 2010 on the Energy Performance of Buildings*; Official Journal of the European Union: Luxembourg, 2010.
5. Santamouris, M. On the Energy Impact of Urban Heat Island and Global Warming on Buildings. *Energy Build.* **2014**, *82*, 100–113. [CrossRef]
6. Mohajerani, A.; Bakaric, J.; Jeffrey-Bailey, T. The Urban Heat Island Effect, Its Causes, and Mitigation, with Reference to the Thermal Properties of Asphalt Concrete. *J. Environ. Manag.* **2017**, *197*, 522–538. [CrossRef] [PubMed]
7. De Cristo, E.; Evangelisti, L.; Battista, G.; Guattari, C.; De Lieto Vollaro, R.; Asdrubali, F. Annual Comparison of the Atmospheric Urban Heat Island in Rome (Italy): An Assessment in Space and Time. *Buildings* **2023**, *13*, 2792. [CrossRef]
8. Carlosena, L.; Ruiz-Pardo, Á.; Rodríguez-Jara, E.Á.; Santamouris, M. Worldwide Potential of Emissive Materials Based Radiative Cooling Technologies to Mitigate Urban Overheating. *Build. Environ.* **2023**, *243*, 110694. [CrossRef]
9. Kuo-Nan, L. *An Introduction to Atmospheric Radiation*, 2nd ed.; Academic Press: Cambridge, MA, USA, 2002; ISBN 0124514510/9780124514515.
10. Kousis, I.; Pigliautile, I.; Pisello, A.L. Intra-Urban Microclimate Investigation in Urban Heat Island through a Novel Mobile Monitoring System. *Sci. Rep.* **2021**, *11*, 9732. [CrossRef] [PubMed]
11. Baldauf, M.; Seifert, A.; Förstner, J.; Majewski, D.; Raschendorfer, M.; Reinhardt, T. Operational Convective-Scale Numerical Weather Prediction with the COSMO Model: Description and Sensitivities. *Mon. Weather. Rev.* **2011**, *139*, 3887–3905. [CrossRef]
12. Jin, L.; Schubert, S.; Hefny Salim, M.; Schneider, C. Impact of Air Conditioning Systems on the Outdoor Thermal Environment during Summer in Berlin, Germany. *Int. J. Environ. Res. Public Health* **2020**, *17*, 4645. [CrossRef] [PubMed]
13. Maronga, B.; Banzhaf, S.; Burmeister, C.; Esch, T.; Forkel, R.; Fröhlich, D.; Fuka, V.; Gehrke, K.F.; Geletič, J.; Giersch, S.; et al. Overview of the PALM Model System 6. *0. Geosci. Model Dev.* **2020**, *13*, 1335–1372. [CrossRef]
14. Anders, J.; Schubert, S.; Sauter, T.; Tunn, S.; Schneider, C.; Salim, M. Modelling the Impact of an Urban Development Project on Microclimate and Outdoor Thermal Comfort in a Mid-Latitude City. *Energy Build.* **2023**, *296*, 113324. [CrossRef]
15. Bergman, L.; Lavine, S.; Incropera, P.; Dewitt, P. *Fundamentals of Heat and Mass Transfer*, 7th ed.; John Wiley & Sons: Hoboken, NJ, USA, 2011; ISBN 13 978-0470-50197-9.
16. Evangelisti, L.; Guattari, C.; Gori, P.; Bianchi, F. Heat Transfer Study of External Convective and Radiative Coefficients for Building Applications. *Energy Build.* **2017**, *151*, 429–438. [CrossRef]
17. Evangelisti, L.; Guattari, C.; Asdrubali, F. On the Sky Temperature Models and Their Influence on Buildings Energy Performance: A Critical Review. *Energy Build.* **2019**, *183*, 607–625. [CrossRef]
18. Adelard, L.; Pignolet-Tardan, F.; Mara, T.; Lauret, P.; Garde, F.; Boyer, H. Sky Temperature Modelisation and Applications in Building Simulation. *Renew. Energy* **1998**, *15*, 418–430. [CrossRef]
19. Alados, I.; Foyo-Moreno, I.; Alados-Arboledas, L. Estimation of Downwelling Longwave Irradiance under All-sky Conditions. *Int. J. Climatol.* **2012**, *32*, 781–793. [CrossRef]
20. Carmona, F.; Rivas, R.; Caselles, V. Estimation of Daytime Downward Longwave Radiation under Clear and Cloudy Skies Conditions over a Sub-Humid Region. *Theor. Appl. Climatol.* **2014**, *115*, 281–295. [CrossRef]
21. Dai, Q.; Fang, X. A New Model for Atmospheric Radiation under Clear Sky Condition at Various Altitudes. *Adv. Space Res.* **2014**, *54*, 1044–1048. [CrossRef]
22. Duarte, H.F.; Dias, N.L.; Maggiotto, S.R. Assessing Daytime Downward Longwave Radiation Estimates for Clear and Cloudy Skies in Southern Brazil. *Agric. Meteorol.* **2006**, *139*, 171–181. [CrossRef]
23. Li, M.; Jiang, Y.; Coimbra, C.F.M. On the Determination of Atmospheric Longwave Irradiance under All-Sky Conditions. *Sol. Energy* **2017**, *144*, 40–48. [CrossRef]
24. *ISO 13790*; Energy Performance of Buildings–Calculation of Energy Use for Space Heating and Cooling. International Organization for Standardization: Geneva, Switzerland, 2008.
25. Swinbank, W.C. Long-wave Radiation from Clear Skies. *Q. J. R. Meteorol. Soc.* **1963**, *89*, 339–348. [CrossRef]
26. Garg, H.P. Treatise on Solar Energy: Fundamental of Solar Energy. JohnWiley & Sons: Chichester, UK, 1982.
27. Ångström, A.K.; Smithsonian Institution. A Study of the Radiation of the Atmosphere, Based upon Observations of the Nocturnal Radiation during Expeditions to Algeria and to California. *Smithson. Misc. Collect.* **1915**, *65*, 1–159.
28. Brunt, D. Notes on Radiation in the Atmosphere. *I. Q. J. R. Meteorol. Soc.* **1932**, *58*, 389–420. [CrossRef]
29. Sloan, R.; Shaw, J.H.; Williams, D. Thermal Radiation from the Atmosphere. *J. Opt. Soc. Am.* **1956**, *46*, 543. [CrossRef]
30. Idso, S.B.; Jackson, R.D. Thermal Radiation from the Atmosphere. *J. Geophys. Res.* **1969**, *74*, 5397–5403. [CrossRef]

31. Berdahl, P.; Martin, M. Emissivity of Clear Skies. *Sol. Energy* **1984**, *32*, 663–664. [CrossRef]
32. Berger, X.; Buriot, D.; Garnier, F. About the Equivalent Radiative Temperature for Clear Skies. *Sol. Energy* **1984**, *32*, 725–733. [CrossRef]
33. Chen, J.; Suetsuna, K.; Yamauchi, F. Isolation and Characterization of Immunostimulative Peptides from Soybean. *J. Nutr. Biochem.* **1995**, *6*, 310–313. [CrossRef]
34. Niemelä, S.; Räisänen, P.; Savijärvi, H. Comparison of Surface Radiative Flux Parameterizations: Part I: Longwave Radiation. *Atmos. Res.* **2001**, *58*, 1–18. [CrossRef]
35. Tang, R.; Etzion, Y.; Meir, I.A. Estimates of Clear Night Sky Emissivity in the Negev Highlands, Israel. *Energy Convers. Manag.* **2004**, *45*, 1831–1843. [CrossRef]
36. Dreyfus, M.G.; Hilleary, D.T. Satellite infrared spectrometer – design and development. *Aerosp. Eng.* **1962**, *21*, 42.
37. Whillier, A. *Design Factors Influencing Solar Collectors in Low Temperature Engineering Applications of Solar Energy*; Ashrae: New York, NY, USA, 1967.
38. Fuentes, M.K. *A Simplified Thermal Model for Flat-Plate Photovoltaic Arrays*; Sandia National Labs: Albuquerque, NM, USA, 1987.
39. Clark, G.; Allen, C. The Estimation of Atmospheric Radiation for Clear and Cloudy Skies. In Proceedings of the 2nd National Passive Solar Conference (AS/ISES), Philadelphia, PA, USA, 16–18 March 1978; pp. 675–678.
40. EnergyPlus. Available online: https://energyplus.net/ (accessed on 23 April 2024).
41. Kasten, F.; Czeplak, G. Solar and Terrestrial Radiation Dependent on the Amount and Type of Cloud. *Sol. Energy* **1980**, *24*, 177–189. [CrossRef]
42. Martin, M.; Berdahl, P. Characteristics of Infrared Sky Radiation in the United States. *Sol. Energy* **1984**, *33*, 321–336. [CrossRef]
43. Bliss, R.W. Atmospheric Radiation near the Surface of the Ground: A Summary for Engineers. *Sol. Energy* **1961**, *5*, 103–120. [CrossRef]
44. ARPALAZIO. Micro-Meteorological Network Data. Available online: https://www.arpalazio.it/rete-micro-meteorologica (accessed on 24 April 2024).
45. MathWorks MATLAB. Available online: https://it.mathworks.com/products/matlab.html (accessed on 24 April 2024).
46. Ruiz, G.R.; Bandera, C.F. Validation of Calibrated Energy Models: Common Errors. *Energies* **2017**, *10*, 1587. [CrossRef]
47. American Society of Heating, Refrigerating and Air Conditioning Engineers (ASHRAE). *Handbook Fundamentals*; American Society of Heating, Refrigerating and Air Conditioning Engineers: Atlanta, GA, USA, 2013; Volume 111.
48. Efficiency Valuation Organization. *International Performance Measurement and Verification Protocol: Concepts and Options for Determining Energy and Water Savings*; Efficiency Valuation Organization: Washington, DC, USA, 2012; Volume I.
49. American Society of Heating, Refrigerating and Air Conditioning Engineers (ASHRAE). *Guideline 14-2002: Measurement of Energy and Demand Savings*; American Society of Heating, Refrigerating and Air Conditioning Engineers: Atlanta, GA, USA, 2002.
50. *ISO 6946:2017*; Building Components and Building Elements—Thermal Resistance and Thermal Transmittance—Calculation Methods. International Organization for Standardization: Geneva, Switzerland, 2017.
51. *ISO 7730:2005*; Ergonomics of the Thermal Environment—Analytical Determination and Interpretation of Thermal Comfort Using Calculation of the PMV and PPD Indices and Local Thermal Comfort Criteria. International Organization for Standardization: Geneva, Switzerland, 2005.